$\gamma\gamma$ interactions with KLOE

Federico Nguyen[1)] (on behalf of the KLOE collaboration)[2)]

INFN Sezione "Roma TRE", Via della Vasca Navale 84, I-00146 Roma, Italy

Abstract Studies of $\gamma\gamma$ interactions are performed with the KLOE detector, without tagging of the outgoing e^+e^-. The data sample is from an integrated luminosity of 240 pb^{-1}. It was collected at the ϕ-factory DAΦNE with e^+e^- beams colliding at $\sqrt{s} \simeq 1$ GeV, below the ϕ resonance peak. We present preliminary results concerning the observation of the $\gamma\gamma \to \eta$ process and the evidence for $\gamma\gamma \to \pi^0\pi^0$ production at low $\pi^0\pi^0$ invariant masses.

Key words e^+e^- collisions, pseudoscalar meson width, π pair production

PACS 12.39.-x, 13.66.Bc

1 Introduction

Most of the e^+e^- colliders have used $\gamma\gamma$ collisions for exploring couplings of pseudoscalar and scalar mesons to photons. In fact, in the process

$$e^+e^- \to e^+e^-\gamma^*\gamma^* \to e^+e^-X\ , \qquad (1)$$

the two photons tend to be quasi-real, with very small probability to produce one vector meson. Therefore, the hadronic state X tends to have $J^{PC}=0^{\pm+}$, $2^{\pm+}$,... quantum numbers [1].

This behaviour implies some approximations when evaluating cross section and event yield, N_{eeX}:

$$N_{eeX} = L_{ee}\int \frac{dF}{dW}\,\sigma_{\gamma\gamma\to X}(W)\,dW\ , \qquad (2)$$

where W is the invariant mass of the two quasi-real photons and L_{ee} is the integrated luminosity. If no cut is applied on the final state $e^\pm$, the Weizsäcker-Williams approximation [2] is used for the $\gamma\gamma$ flux function, dF/dW, with E_b being the $e^\pm$ beam energy:

$$\frac{dF}{dW} = \frac{1}{W}\left(\frac{2\alpha}{\pi}\right)^2\left(\ln\frac{E_b}{m_e}\right)^2\left((z^2+2)^2\ln\frac{1}{z} - (1-z^2)(3+z^2)\right),\quad z=\frac{W}{2E_b} \qquad (3)$$

Fig. 1 shows the flux function as a function of the $\gamma\gamma$ center of mass energy, where threshold openings of different hadronic states are indicated.

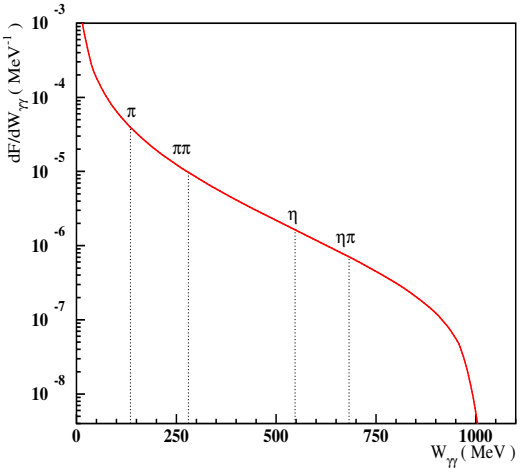

Fig. 1. Flux function of $\gamma\gamma$ collisions at $\sqrt{s}=1$ GeV.

Received 25 January 2010

1) E-mail: nguyen@fis.uniroma3.it

2) F. Ambrosino, A. Antonelli, M. Antonelli, F. Archilli, P. Beltrame, G. Bencivenni, C. Bini, C. Bloise, S. Bocchetta, F. Bossi, P. Branchini, G. Capon, T. Capussela, F. Ceradini, P. Ciambrone, E. De Lucia, A. De Santis, P. De Simone, G. De Zorzi, A. Denig, A. Di Domenico, C. Di Donato, B. Di Micco, M. Dreucci, G. Felici, S. Fiore, P. Franzini, C. Gatti, P. Gauzzi, S. Giovannella, E. Graziani, M. Jacewicz, W. Kluge, J. Lee-Franzini, M. Martini, P. Massarotti, S. Meola, S. Miscetti, M. Moulson, S. Müller, F. Murtas, M. Napolitano, F. Nguyen, M. Palutan, A. Passeri, V. Patera, P. Santangelo, B. Sciascia, T. Spadaro, L. Tortora, P. Valente, G. Venanzoni, R. Versaci, G. Xu

Table 1. Pseudoscalar meson production in $\gamma\gamma$ collisions: cross section values at $\sqrt{s}=1$ GeV.

process	σ/pb
$e^+e^- \to e^+e^-\pi^0$	266
$e^+e^- \to e^+e^-\eta$	43
$e^+e^- \to e^+e^-\eta'$	3.3

For the particular case of $e^+e^- \to e^+e^-X$, with $X=\pi^0,\eta,\eta'$, the narrow width approximation simplifies the cross section formula [2]:

$$\sigma_{e^+e^-\to e^+e^-X} = \frac{16\alpha^2\Gamma_{X\gamma\gamma}}{m_X^3}\left(\ln\frac{E_b}{m_e}\right)^2 \times \left((z^2+2)^2\ln\frac{1}{z}-(1-z^2)(3+z^2)\right), \quad z=\frac{m_X}{2E_b} \quad (4)$$

with m_X and $\Gamma_{X\gamma\gamma}$ being respectively the mass and the radiative partial width of the pseudoscalar meson. Table 1 shows the cross section values for producing pseudoscalar mesons at $\sqrt{s}=1$ GeV. Previous experiments measuring the $\gamma\gamma$ cross section for the pseudoscalar meson production, took data at a center of mass energy $7<\sqrt{s}<35$ GeV. A low energy e^+e^- factory, such as DAΦNE, compensates the small cross section value with the high luminosity.

2 $\gamma\gamma$ collisions with KLOE at DAΦNE

DAΦNE is an e^+e^- collider designed to operate at the center of mass energy $\sqrt{s}\simeq 1.02$ GeV, namely the ϕ meson mass. It has provided to the KLOE experiment an integrated luminosity of about 2.5 fb^{-1} on peak of the ϕ meson up to year 2005 and also about 240 pb^{-1} at $\sqrt{s}\simeq 1$ GeV, in year 2006.

The KLOE detector consists of a large volume cylindrical drift chamber [5], 3.3 m length and 2 m radius, surrounded by a calorimeter [6] made of lead and scintillating fibers. The detector is inserted in a superconducting coil producing an axial field B=0.52 T. Charged particle momenta are reconstructed with resolution $\sigma_p/p\simeq 0.4\%$ ($\sigma_p/p\simeq 1\%$) for large (small) angle tracks coming from the collision point. Energy clusters are reconstructed from calorimeter cells close in space and in time with energy and time resolution of $\sigma_E/E=5.7\%/\sqrt{E(\mathrm{GeV})}$ and $\sigma_t=57$ ps$/\sqrt{E(\mathrm{GeV})}\oplus 100$ ps. The trigger system [7] requires at least two energy deposits above threshold in the calorimeter, not in the same end cap: the threshold is 50 MeV for the barrel and 150 MeV for each end cap.

Since $e^\pm$ in the final state of $e^+e^- \to e^+e^-X$ go undetected along the beam pipe, it is important to use Monte Carlo, MC, generators with formulae beyond the Weizsäcker–Williams approximation [3, 4]. In particular, in the data analysis the complete phase space simulation is used for evaluating the selection efficiency. For example, Fig. 2 shows the p_T distribution of the η produced in $e^+e^- \to e^+e^-\gamma^*\gamma^* \to e^+e^-\eta$: the complete 3-body phase space is compared with the Weizsäcker–Williams approximation.

The sample used for the present analyses consists of data taken at $\sqrt{s}\simeq 1$ GeV, which allows to suppress background from ϕ decays (see Table 2 in the following). Moreover, a dedicated algorithm has been developed for filtering this kind of events, having significant missing energy:

1) at least 2 photons with energy $E>15$ MeV and polar angle $20^\circ<\theta<160^\circ$, the most energetic one with $E>50$ MeV;

2) fraction of energy carried by photons, $R=(\sum_\gamma E_\gamma)/E_{\mathrm{calo}}>0.3$;

3) total energy in the calorimeter, E_{calo}, $200<E_{\mathrm{calo}}<900$ MeV.

Where the latter requirement rejects low energy background and the high rate processes $e^+e^- \to e^+e^-$ and $e^+e^- \to \gamma\gamma$.

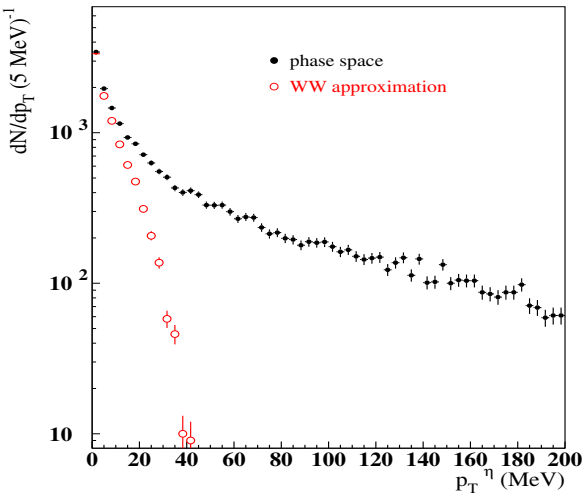

Fig. 2. Comparison between the complete 3-body phase space and the Weizsäcker–Williams approximation for the p_T distribution of the η in $e^+e^- \to e^+e^-\eta$ events.

3 Observation of $e^+e^- \to e^+e^-\eta \to e^+e^-\pi^+\pi^-\pi^0$ events

The η radiative width, $\Gamma_{\eta\gamma\gamma}$, is usually extracted from the measurement of the $e^+e^- \to e^+e^-\eta$ cross section, using the formula in Eq. (4). This formula is obtained neglecting the $\eta\gamma\gamma$ transition form factor, $F(q_1^2,q_2^2)$, depending on the momentum transfers of

the photons, q_1 and q_2:

$$\sigma_{\gamma\gamma\to\eta}(q_1,q_2) \propto \frac{\Gamma_{\eta\gamma\gamma}}{m_\eta}\,\delta((q_1+q_2)^2-m_\eta^2)\,|F(q_1^2,q_2^2)|^2 \ .$$

Recent emphasis is put on measuring these form factors, for their role in constraining models [8] used to evaluate the hadronic light-by-light contribution to the magnetic anomaly of the muon.

The selection of candidate $\eta \to \pi^+\pi^-\pi^0$ events – where $BR(\eta \to \pi^+\pi^-\pi^0) = 22.73\%$ – consists of:

A) two and only two photons, constrained to originate from a π^0 decay;

B) two tracks with opposite curvature coming from the collision point, with the best quality parameters;

C) sum of the track momenta $|\vec{p}_1|+|\vec{p}_2| < 700$ MeV, to suppress higher momentum values, typical of $e^+e^- \to \pi^+\pi^-\pi^0$ or $e^+e^- \to \omega(\to \pi^+\pi^-\pi^0)\pi^0$.

The charged pion mass is assigned to the two tracks and a least squares function, χ^2_η, based on Lagrange multipliers imposes that the three pions come from an η decay. Therefore most background events are suppressed, except for the irreducible process $e^+e^- \to \eta\gamma \to \pi^+\pi^-\pi^0\gamma$, with the monochromatic photon lost in the beam pipe. For these events, the requirement A) constrains the 3π system to be emitted with longitudinal momentum $p_L \simeq 350$ MeV and recoil missing mass $M_{miss} \simeq 0$. On the other hand, signal events are characterized by the following parabolic relation between M^2_{miss} and p_L:

$$M^2_{miss} \approx s + m_\eta^2 - 2E_T\sqrt{s} - \frac{p_L^2}{E_T}\sqrt{s} \qquad (5)$$

where

$$E_T = \sqrt{p_T^2 + m_\eta^2} \approx m_\eta$$

with negligible transverse momentum, a continuous spectrum in p_L, $-350 < p_L < 350$ MeV, and high M^2_{miss} values. Fig. 3 shows the parabolic relation both on data (top panel), where the spots related to $\eta\gamma$ events are visible, and on signal Monte Carlo events (bottom panel).

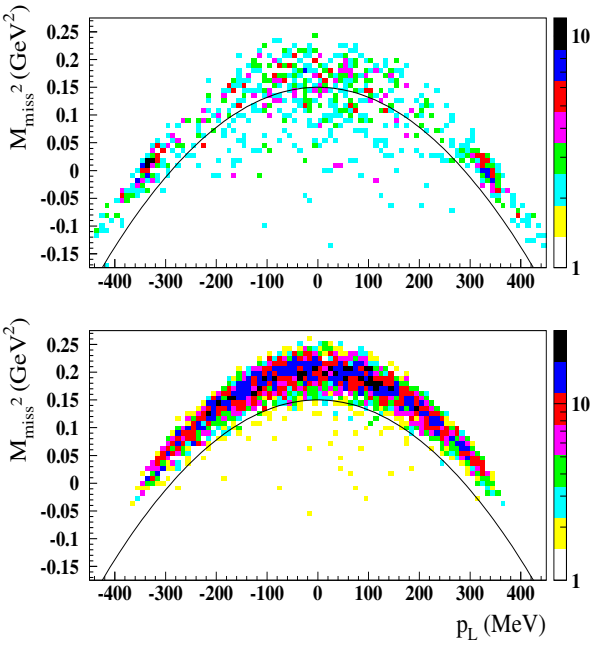

Fig. 3. Correlation between longitudinal momentum and recoil missing mass of the 3π system for data (top) and signal MC (bottom). The solid line is the applied parabola cut.

Further criteria are applied for suppressing processes with photons and e^+e^- as tracks in the final state, such as $\eta(\to 3\pi^0)\gamma$ with photon conversion or radiative Bhabha events, $e^+e^-\gamma(\gamma)$.

Table 2. Values of cross section, selection efficiencies and fit results for the $\gamma\gamma \to \eta$ signal and background processes.

	signal	$\eta\gamma$	$\omega\pi^0$	$\pi^+\pi^-\pi^0$	K^+K^-	K_SK_L	$e^+e^-\gamma(\gamma)$
σ/nb	0.043	0.23 [9]	5.7 [10]	30 [11]	8.6 [12, 13]	2.0 [12]	~ 400
ε	20%	9.2×10^{-3}	6.3×10^{-5}	1.5×10^{-5}	1.9×10^{-5}	1.7×10^{-5}	$\mathcal{O}(10^{-7})$
$N_{fit}(p_L)$	646	442	87	101	46	14	286
$N_{fit}(M^2_{miss})$	625	442	87	101	46	14	303

Event distributions in p_L and M^2_{miss} from data are independently fitted with the superposition of MC shapes for signal and background. Table 2 shows the expected cross section, the selection efficiency and the event yields after fit to the signal and relevant background distributions. Both fits show the same yields for the background processes and more than 600 $e^+e^- \to e^+e^-\eta \to e^+e^-\pi^+\pi^-\pi^0$ events. Fig. 4 shows that both fits have good χ^2/dof values.

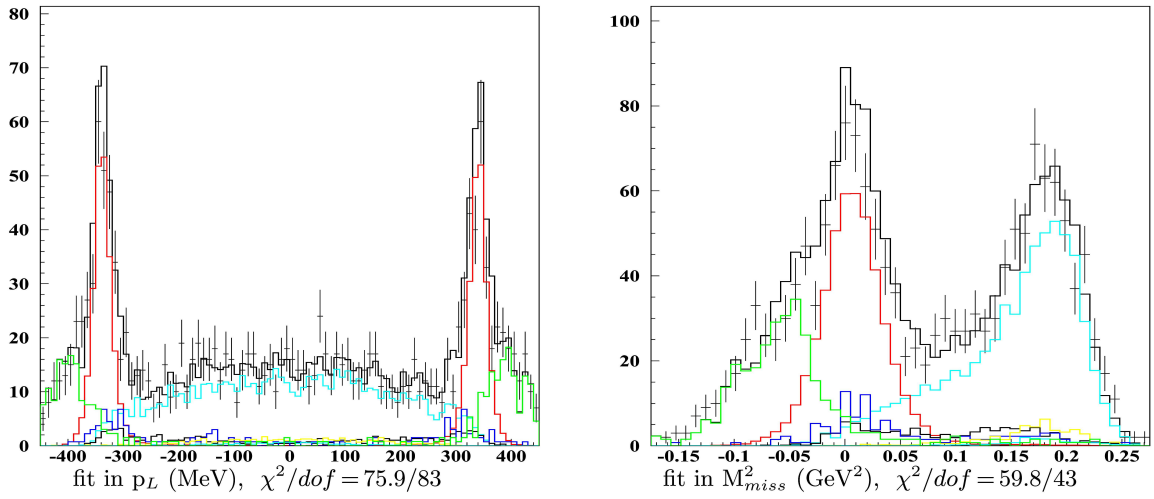

Fig. 4. Fits in dN/dp_L (left) and $dN/dM^2_{\rm miss}$ (right): signal (cyan), $\eta\gamma$ (red) and $e^+e^-\gamma(\gamma)$ (green) are visible.

4 Search for $e^+e^- \to e^+e^-\pi^0\pi^0$ events

The interest in this process is given by the $\sigma(600) \to \pi\pi$ contribution [14]. The determination of the $\sigma\gamma\gamma$ coupling can be compared with that of pseudoscalar or other scalar states to clarify their quark structure.

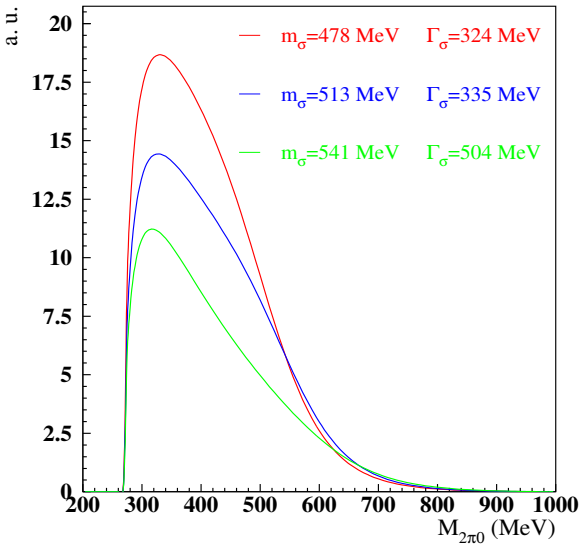

Fig. 5. Expected $M_{2\pi^0}$ distribution for $\gamma\gamma \to \pi^0\pi^0$ events, according to the specified [15–17] values of $\sigma(600)$ mass and width.

From the experimental point, the $\pi^0\pi^0$ is preferred with respect to the $\pi^+\pi^-$ channel because of the background from initial state radiation events, $e^+e^- \to \rho(\to \pi^+\pi^-)\gamma$ with photon lost in the beam pipe, from the $\gamma\gamma \to \mu^+\mu^-$ reaction (almost an order of magnitude larger) and because of the interference with the QED process $\gamma\gamma \to \pi^+\pi^-$. Finally, the selection rules for $\gamma\gamma \to \pi^0\pi^0$ forbid any interference with vector or pseudoscalar states with mass close to the $\sigma(600)$. Examples of the $\pi^0\pi^0$ invariant mass shape, $M_{\pi^0\pi^0}$, expected in $\gamma\gamma \to \sigma$ production for different σ parameters, are shown in Fig. 5, where a Breit-Wigner function is folded with the $\gamma\gamma$ flux function.

The main requirement of the data analysis consists of four and only four photons, used to evaluate the following variable:

$$\chi^2_{\pi\pi} = \frac{(M_{\gamma_i\gamma_j} - m_{\pi^0})^2}{\sigma^2_{\gamma_i\gamma_j}} + \frac{(M_{\gamma_k\gamma_l} - m_{\pi^0})^2}{\sigma^2_{\gamma_k\gamma_l}},$$

where $\sigma_{\gamma\gamma}$ is the resolution function of the two photons invariant mass $M_{\gamma\gamma}$. Fig. 6 shows that the cut $\chi^2_{\pi\pi} < 4$ selects 4-photon events originated from $2\pi^0$ decays. Other selection criteria are applied:

1) photon energy fraction, $(\sum_\gamma E_\gamma)/E_{\rm calo} > 0.8$;

2) 4-photon transverse momentum, $p_{\rm T} < 80$ MeV;

3) no tracks reconstructed in the drift chamber;

4) energy sum of the 2 least energetic photons, $\sum_{2\gamma_{\rm min}} E_\gamma > 60$ MeV.

About 10^4 events fulfill these requirements, with a signal efficiency of about 20% estimated from Monte Carlo. The spectrum in the 4-photon invariant mass, $M_{4\gamma}$, is compared with expected background yields. These are based on the present knowledge of the cross sections and Monte Carlo efficiency evaluations.

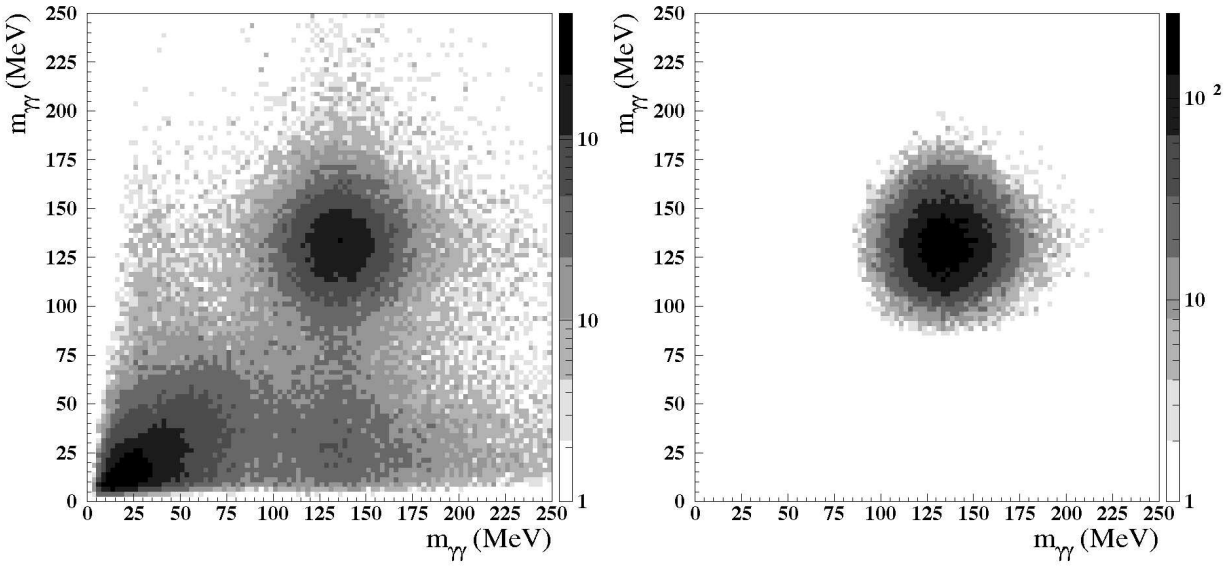

Fig. 6. Distribution of the $\gamma\gamma$ invariant mass for the combinations with minimum $\chi^2_{\pi\pi}$ value, before (left) and after (right) applying the $\chi^2_{\pi\pi} < 4$ selection.

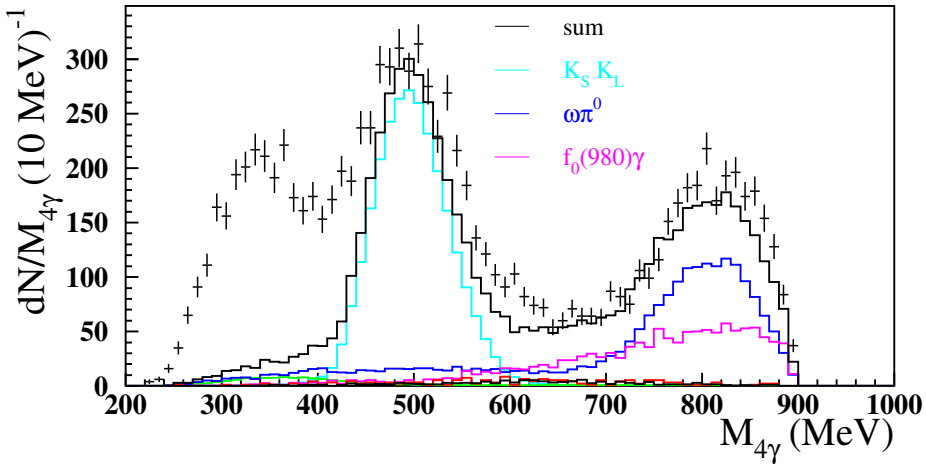

Fig. 7. Spectrum of the 4-photon invariant mass, compared with the sum of the expected backgrounds. Peak of the $K_S \to \pi^0\pi^0$ decay and structures related to other processes with two π^0 are visible: $\omega(\to \pi^0\gamma)\pi^0$ and $f_0(980)(\to 2\pi^0)\gamma$. The cut on $M_{4\gamma} < 900$ MeV is explained by the requirement on the total energy in the calorimeter, $E_{\rm calo} < 900$ MeV.

Table 3. Cross sections, selection efficiencies and event yields of the background processes.

process	ε (%)	σ/nb	$\varepsilon\sigma\mathcal{L}$	fraction
$K_S(\to 2\pi^0)K_L$	0.56	2.0	2 682	0.26
$\omega(\to \pi^0\gamma)\pi^0$	1.55	0.55	2 045	0.20
$f_0(980)(\to 2\pi^0)\gamma$	2.58	0.17	1 052	0.10
$\eta(\to 3\pi^0)\gamma$	0.18	0.33	142	0.014
$e^+e^- \to 2\gamma(2\gamma)$	0.002	360	166	0.016

Table 3 shows the background processes which after analysis cuts give a significant contribution to the $M_{4\gamma}$ spectrum obtained from data. Efficiencies from Monte Carlo, together with expected event yields are also shown. Besides the several reactions with at least a genuine $\pi^0\pi^0$ pair, there is also contamination from $e^+e^- \to 2\gamma(2\gamma)$ events. These mainly consist of events with annihilation into 3 photons plus an accidental cluster, or one of the 3 photons is reconstructed as two (or more) clusters, which survive selection cuts due to the high cross section production.

After the selection cuts, the final $M_{4\gamma}$ spectrum is shown in Fig. 7. From the plot, an excess (with respect to the backgrounds discussed above) of about 4000 events is evident at low $M_{4\gamma}$ values, consis-

tent in shape with expectations (see Fig. 5) from $e^+e^- \to e^+e^-\pi^0\pi^0$ events. The precise yield estimate depends on assumptions for the background processes. Systematic study of the differential cross section and understanding of the $\sigma \to \pi\pi$ contribution are in progress.

5 Conclusions

Using an integrated luminosity of 240 pb^{-1} of data collected at DAΦNE, operating at $\sqrt{s} \simeq 1$ GeV, the following preliminary results in $\gamma\gamma$ analyses are achieved:

1) unambiguous signature of both $\gamma\gamma \to \eta$ and $\gamma\gamma \to \pi^0\pi^0$ events, without any $e^\pm$ tagger;

2) $\gamma\gamma \to \eta$ events are observed through the $\eta \to \pi^+\pi^-\pi^0$ channel;

3) from the same data sample, an exploratory research shows a structure at small values of the $M_{4\gamma}$ spectrum, where the process $e^+e^- \to e^+e^-\pi^0\pi^0$ is expected.

These results are encouraging also in view of the forthcoming data taking campaign of the KLOE-2 project [18], when both low and high energy $e^\pm$ tagging devices will be available.

References

1 YANG C N. Phys. Rev., 1950, **77**: 242
2 Brodsky S J, Kinoshita T, Terazawa H. Phys. Rev. D, 1971, **4**: 1532
3 Nguyen F, Piccinini F, Polosa A D. Eur. Phys. J. C, 2006, **47**: 65
4 Nguyen F. Acta Phys. Polon. B, 2007, **38**: 2967
5 Adinolfi M et al (KLOE collaboration). Nucl. Instrum. Meth. A, 2002, **488**: 51
6 Adinolfi M et al (KLOE collaboration). Nucl. Instrum. Meth. A, 2002, **482**: 364
7 Adinolfi M et al (KLOE collaboration). Nucl. Instrum. Meth. A, 2002, **492**: 134
8 Nyffeler A. These Proceedings
9 Achasov M N et al (SND collaboration). Phys. Rev. D, 2007, **76**: 077101
10 Ambrosino F et al (KLOE collaboration). Phys. Lett. B, 2008, **669**: 223
11 Achasov M N et al (SND collaboration). Phys. Rev. D, 2002, **66**: 032001
12 Achasov M N et al (SND collaboration). Phys. Rev. D, 2001, **63**: 072002
13 Akhmetshin R R et al (CMD-2 collaboration). Phys. Lett. B, 2008, **669**: 217
14 Amsler C et al (Particle Data Group). Phys. Lett. B, 2008, **667**: 1
15 Aitala E M et al (E791 collaboration). Phys. Rev. Lett., 2001, **86**: 770
16 Muramatsu H et al (CLEO collaboration). Phys. Rev. Lett., 2002, **89**: 251802; 2003, **90**: 059901
17 Ablikim M et al (BES collaboration). Phys. Lett. B, 2004, **598**: 149
18 Venanzoni G. These Proceedings